Theor Appl Genet (2008) 116:465–479
DOI 10.1007/s00122-007-0683-1

ORIGINAL PAPER

A guanylyl cyclase-like gene is associated with Gibberella ear rot resistance in maize (*Zea mays* L.)

J. Yuan · M. Liakat Ali · J. Taylor · J. Liu · G. Sun · W. Liu · P. Masilimany · A. Gulati-Sakhuja · K. P. Pauls

Received: 28 November 2006 / Accepted: 21 November 2007 / Published online: 12 December 2007
© Springer-Verlag 2007

Abstract Gibberella ear rot, caused by the fungal pathogen *Fusarium graminearum* Schwabe, is a serious disease of maize (*Zea mays* L.) grown in northern climates. The infected maize grain contains toxins that are very harmful to livestock and humans. A maize gene that encodes a putative 267-amino acid guanylyl cyclase-like protein (ZmGC1) was characterized and shown to be associated with resistance to this disease. The putative ZmGC1 amino acid sequence is 53% identical and 65% similar to AtGC1, an *Arabidopsis* guanylyl cyclase. The *Zmgc1* coding sequence is nearly identical in a Gibberella ear rot-resistant line (CO387) and a susceptible line (CG62) but several nucleotide sequence differences were observed in the UTRs and introns of the two alleles. Using a 463 bp probe derived from the CG62 allele of *Zmgc1* and a recombinant inbred (RI) mapping population developed from a CG62 × CO387 cross, six *Zmgc1* restriction fragment length polymorphism (RFLP) fragments (ER1_1, ER1_2, ER1_3, ER1_4, ER1_5, and ER5_1) were mapped on maize chromosomes 2, 3, 7, and 8. Markers ER1_1 and ER5_1 on chromosomes 7 and 8, respectively, were significantly associated with Gibberella ear rot resistance, each in three different environments. The amount of *Zmgc1* transcript in ear tissues increased more quickly and to a greater extent in the resistant genotype compared to the susceptible genotype after inoculation with *F. graminearum*. *Zmgc1* is the first guanylyl cyclase gene characterized in maize and the first gene found to be associated with Gibberella ear rot resistance in this plant.

Communicated by T. Tai.

J. Yuan · M. L. Ali · J. Taylor · J. Liu · G. Sun · W. Liu · P. Masilimany · A. Gulati-Sakhuja · K. P. Pauls (✉)
Department of Plant Agriculture,
University of Guelph, Guelph, ON, Canada, N1G 2W1
e-mail: ppauls@uoguelph.ca

J. Yuan
Department of Plant Biology,
Southern Illinois University, Carbondale, IL 62901, USA

M. L. Ali
Department of Agronomy and Horticulture,
University of Nebraska, Lincoln, NE 68583, USA

Introduction

Fusarium graminearum Schwabe causes Gibberella ear rot disease in maize (*Zea mays* L.) (Sutton 1982) as well as head blight in wheat and barley (McMullen et al. 1997). Gibberella ear rot is characterized by a reddish–white mold that usually begins at the tip of the infected maize ear and can grow to cover the entire ear (Sutton 1982). Infected grain is contaminated with mycotoxins, such as deoxynivalenol (vomitoxin) and zearalenone (Molto et al. 1997; Greenhalgh et al. 1983). Contaminated grain fed to livestock (especially swine) induces emesis characterized by vomiting, feed refusal, and decreased weight gain (Christensen and Meronuck 1986). In addition, birth defects have been observed in ruminants exposed to mycotoxins (Mirocha et al. 1976). Resistance to ear rot in maize is quantitatively inherited, specific to the mode of fungal entry (silk channels or kernel wounds) and highly influenced by the environment (Sutton 1982; Chungu et al. 1996; Ali et al. 2005). There are two types of resistance to Gibberella ear rot identified in maize (Chungu et al. 1996; Reid et al. 1992). Silk resistance is considered to prevent the fungus from invading through silk channel down to the kernels. Kernel resistance blocks the spread of the fungus from kernel to kernel when the pathogen bypasses silk channels or overcomes silk resistance barriers (Chungu et al. 1996).

Markers linked to disease resistance genes can potentially be used for marker-assisted selection in breeding programs (Young 1999; Yousef and Juvik 2001). Many reports describe tight linkages between molecular markers and genetic loci affecting simply inherited or quantitative traits for maize and other cereals (e.g. Stuber et al. 1992; Tanksley and Nelson 1996; Xiao et al. 1996). Pe et al. (1993) identified several quantitative trait loci (QTL) for resistance to stalk rot caused by *F. graminearum* in corn on chromosomes 1, 2, 4, 5, and 10. Dehydrodimers of ferulic acid in maize grain pericarp and aleurone were found to be related to resistance to Gibberella ear rot (Bily et al. 2003).

Recently, we identified several QTL for resistance to Gibberella ear rot in maize using a mapping population of recombinant inbred (RI) lines segregating for kernel and silk resistance to *F. graminearum* infection (Ali et al. 2005). One of the markers used in our study, BC324-1400 (about 1200 bp), was identified by random amplified polymorphic DNA (RAPD) analysis and shown to be significantly associated with kernel and silk resistance. The fragment was cloned and sequenced and was found to contain a sequence with homology to a guanylyl cyclase (EC 4.6.1.2) gene from *Arabidopsis* (data not shown).

Guanylyl cyclases (EC 4.6.1.2, also called guanylate cyclases; GCs) catalyze the formation of guanosine 3′, 5′-cycline monophosphate (cGMP) from guanosine 5′-triphosphate (GTP). In animals, cGMP functions as a key messenger in phototransduction, nitric oxide (NO) signaling, and arterial natriuretic peptide signaling (Garbers and Lowe 1994). In plants, cGMP is required for signal transduction (Bowler et al. 1994), plant defense (Durner et al. 1998), and ion channel regulation (Dzeja et al. 1999). Animal GCs exist in soluble and transmembrane forms (Lucas et al. 2000). Soluble GCs function as heterodimers (a and b subunits) with one catalytic domain contributed by each of the two subunits. They contain heme as a prosthetic group and are the principal effectors of the gaseous messenger NO (Ludidi and Gehring 2003).

GCs are distributed across the animal kingdom (Hurley 1998; Schaap 2005). At least 29 GC genes have been identified in nematode (*Caenorhabditis elegans*) (Yu et al. 1997) while only a single plant GC has been functionally identified to date (Ludidi and Gehring 2003). The *Arabidopsis* GC, called AtGC1 (AAM51559, Ludidi and Gehring 2003), was identified by searching the *Arabidopsis* proteome with a motif based on conserved amino acids in the catalytic centers of annotated GCs. AtGC1 also contains the adjacent glycine-rich domain typical for GCs. However, unlike animal GCs, the catalytic domain of AtGC1 is located in the N-terminal portion. AtGC1 has the arginine or lysine that is involved in hydrogen bonding with guanine and the cysteine that confers substrate specificity for GTP that are found in other GCs (Thompson and Garbers 1995). Expression of AtGC1 in bacteria raised the cGMP concentration 2.5 fold in a NO independent manner. The purified recombinant AtGC1 demonstrated Mg^{2+}-dependent GC activity in vitro and had some adenylyl cyclase activity when assayed with ATP as substrate in the absence of GTP. Tests of in vitro catalytic activity showed that the recombinant AtGC1 could function either as a monomer or homo-oligomer (Ludidi and Gehring 2003).

NO, cGMP, and cADP are activators of phenylalanine ammonia lyase (PAL) and pathogenesis related-1 (PR-1) gene expression. PAL expression has been associated with resistance to infection by fungal pathogens in many plant species (Durner et al. 1998; McDowell and Woffenden 2003). Durner et al. (1998) demonstrated that cGMP functions as a second messenger in the induction of PAL by exogenous NO. Further, cGMP can stimulate the induction of genes encoding chalcone synthase that are associated with the formation of phenylpropanoid-derived pigments and can initiate anthocyanin biosynthesis in soybean (Bowler et al. 1994). Therefore, cGMP is associated with the synthesis of phenylpropanoid products and defense responses. In addition, reactive oxygen intermediates induce hypersensitive cell death by raising cytosolic calcium (Levine et al. 1996) and NO can reduce the threshold for calcium signaling by modulating cGMP-gated ion channels (Berridge 1993). Tobacco pathogenesis related-protein 1 (PR1) has antifungal activities and is a biomarker of plant response to pathogens (Durner et al. 1998; Ryals et al. 1996). In plants, cGMP is involved in modulating PR-1 gene expression (Bowler et al. 1994).

Our objective was to further characterize the molecular basis of resistance to Gibberella ear rot disease in corn by testing the cosegregation of sequences homologous to a GC sequence found in the RAPD marker BC324-1400 with resistance and by comparing the accumulation of GC messages in inoculated resistant and susceptible corn lines.

Materials and methods

Plant materials

A F_5 recombinant inbred (RI) population ($n = 144$) was derived by single seed descent from a cross between the inbred lines, CG62 and CO387 (Ali et al. 2005). CG62 was developed at the University of Guelph from Pioneer 3902 (Lee et al. 2001) and is susceptible to *F. graminearum* after silk or kernel inoculation (Ali et al. 2005). CO387, developed at Agriculture and Agri-Food Canada (AAFC, Ottawa, ON, Canada), has resistance to Gibberella ear rot following silk or kernel inoculation (Reid et al. 1994; Reid and Hamilton 1996). This F_5 population was previously

genotyped with 162 molecular markers and phenotyped for Gibberella ear rot disease in four environments, resulting in the identification of 18 QTL for resistance to *F. graminearum* (Ali et al. 2005).

Nucleic acid isolation and *F. graminearum* inoculation

Genomic DNA samples for cloning the *Zmgc1* gene and gene mapping were obtained from young leaves of the two parental inbred lines (CG62 and CO387) and 144 RI lines (F_5 generation). The leaves were harvested from field grown plants, freeze–dried, and ground to fine powder. DNA was extracted from the powdered leaf material using the cetyltrimethyl ammonium bromide (CTAB) method (Hoisington et al. 1994).

To collect RNA samples, seeds of the parental lines were germinated in trays (30 × 30 × 5 cm) containing commercial soil mixture (Terra-lite Redi-earth, WR Grace & Co, Canada Ltd, Ajax, ON, Canada). Seedlings were transferred to pots containing Turface quick-dry® (Hobbs & Hopkins Ltd, OR, USA) and maintained in a greenhouse at 25/20°C (day/night) with a 16 h light (800 microeinsteins/m^2/s) and 8 h dark photoperiod. Twenty-six plants per genotype were arranged following a completely randomized design and ears on each plant were inoculated with *F. graminearum* microconidia as described below. Ear samples from each inbred were obtained at 0, 1, 4, 24, 48, 120, and 240 h after inoculation. The sampling was repeated three times for each genotype. The plant tissues were immediately frozen in liquid nitrogen and kept at −80°C. Total RNA was isolated using the RNeasy plant mini kit (Qiagen, Mississauga, ON, Canada) in combination with DNase treatment using the RNase-free DNase kit (Qiagen GmbH, Hilden, Germany) according to the manufacturer's instruction.

All isolates were obtained from the Ridgetown College, University of Guelph and were previously isolated from naturally infected maize ears. A microconidial suspension of *F. graminearum* in this study was prepared as described (Reid and Hamilton 1996). Isolates were cultured on potato dextrose agar medium (PDA, Difco, Detroit, MI, USA). Plates were incubated at 25°C under continuous fluorescent light (900 microeinsteins/m^2/s) and conidia were harvested from eight to 10-day-old cultures by flooding the plates with sterile distilled water. The density of the inoculum was adjusted to 2.5×10^5 conidia ml^{-1} with sterile distilled water. Each plant was inoculated by injecting 2 ml of the conidial suspension into the silk channel of the primary ear using a syringe with an 18 gauge needle. After inoculation, plants were placed in a greenhouse with a 16 h light (800 microeinsteins/m^2/s) and 8 h dark photoperiod at 25/20°C (day/night). Humid conditions were maintained by misting twice a day for 4 weeks.

RAPD, genome walking, RACE, and sequence analyses

In order to clone the BC324-1400 fragment, which was significantly associated with the ear rot resistance in maize (Ali et al. 2005), the RAPD primer BC324 (5′-ACAGGGAACG-3′) was used for the initial amplification of genomic DNA as described in Ali et al. (2005). A 1200-bp fragment was amplified from CG62 genomic DNA in 20 µl PCR containing 30 ng template DNA, PCR buffer (1X), 0.5 U of *Taq* polymerase (Invitrogen, Burlington, ON, Canada), 2 mM $MgCl_2$, 0.2 mM each of dATP, dCTP, dTTP and dGTP, and 15 ng of the RAPD primer. Amplifications were performed in a DNA Thermo-cycler (MJ Research Inc, Scarborough, ON, Canada) programmed for 41 cycles of 1 min at 94, 36 and 72°C. Following amplification, the samples were electrophoresed through 0.8% agarose gels, stained with 0.5 µg/ml ethidium bromide and visualized under UV light. The DNA fragment was purified with a Qiagen gel purification kit (Qiagen, Mississauga, ON, Canada), cloned using an Invitrogen TOPO TA cloning kit (Invitrogen, Burlington, ON, Canada), and introduced into *Escherichia coli* One-Shot competent cells according to the manufacturer's instructions (Invitrogen, Burlington, ON, Canada). Several clones were picked and plasmid DNA was isolated with a Qiagen Miniprep Kit (Qiagen, Mississauga, ON, Canada). The cloned fragments were sequenced with a CEQ2000 sequencer (Beckman-Coulter, Fullerton, CA, USA) after labeling with a DTCS Quick Start sequencing kit (Beckman-Coulter, Fullerton, CA, USA).

A number of additional primers used for the following experiments were synthesized by Sigma-Aldrich (Sigma-Aldrich, Mississauga, ON, USA) and Laboratory Services at University of Guelph (Guelph, ON, Canada). The universal GenomeWalker™ kit (BD Biosciences, Palo Alto, CA, USA) was used to obtain sequences adjacent to the cloned RAPD fragment. Several genomic DNA libraries were constructed by digesting with four different restriction enzymes (in 100 µl reactions containing 3 µg of genomic DNA, 80 units of restriction enzyme and 1X restriction buffer) and adaptors were ligated to the ends of the fragments according to manufacturer's instructions. Several GC rich gene specific primers (26–30 bp) were designed for genome walking in both directions based on sequence information from the BC324-1400. The outer adaptor primer (AP1) provided in the kit, a gene-specific primer GSP1 (5′-GGATTTCCGGGCCTCGTCCAAGCTCTTCA-3′) and DNA of each of the libraries were used for the primary PCR reaction. The primary PCR product was used as template for a secondary PCR with the nested adaptor primer (AP2) and a nested gene-specific primer (GSP2, 5′-AGCGGCAGCAAAAGGCTCTGCTGACCTTG-3′). A single, major PCR product from at least one of the four libraries was gel purified using a gel purification kit (Invitrogen, Burlington, ON,

Canada), cloned using the TOPO TA cloning kit (Invitrogen, Burlington, ON, Canada) and sequenced as described above. Each of the DNA fragments began in a known sequence, corresponding to GSP2, and extended into the unknown adjacent genomic DNA. The new sequence information was used to design new gene specific primers for further genome walking.

In order to clone and sequence the 3′- and 5′- ends of the *Zmgc1* gene transcript, a rapid amplification of cDNA end (RACE) procedure was performed as detailed in the instructions for the SMART™ RACE cDNA amplification kit (BD Biosciences, San Jose , CA, USA). The primers for RACE were derived from a consensus sequence between the sequence from genome walking and a homologous cDNA in GenBank (AY110155.1). The gene-specific primers used for 5′-RACE and 3′-RACE were 5′-ATTTG CGGGCCTCGTCCAAGCTCTTCA-3 and 5′-ACAACA GCACAACGATGAGCCTGACTAC-3′, respectively. The PCR mixture of 25 µl contained: 2.0 µl of template 3′-end or 5′-end cDNA, 2.5 µl universal primer A mix, 2.5 µl 10 µM GSP, and 18 µl master mix which contained 14.5 µl PCR-grade water, 2.5 µl 10X BD Advantage PCR buffer, 0.5 µl dNTP mix (10 mM), and 0.5 µl 50X BD advantage 2 polymerase mix. Amplifications were performed in a thermo-cycler programmed for 30 cycles of 30 s at 94°C, 30 s at 68°C and 3 min at 72°C. Following amplification, the samples were subjected to electrophoresis in 0.8% agarose gels, stained with 0.5 µg/ml ethidium bromide, and visualized under UV light. The DNA fragment was gel purified, cloned and sequenced as described above.

The full-length *Zmgc1* sequence was determined by piecing together the sequences of the RAPD fragment, the RACE products, expressed sequence tags in GenBank (CO531826 and AY110155.1), and the genome walking fragments with CAP3 (Huang and Madan 1999) and Sequencher (Version 4.05, Gene Codes Corporation, Ann Arbor, MI, USA) programs. Primers *Zmgc1*-F 5′-GTGTC-CACCGCGCTCGCCCCCTGCT -3, and *Zmgc1*-R 5′-AGAGGAGCATGATTTTAATTTTA-3′ were used to obtain fragments encompassing the complete open reading frame of the *Zmgc1* gene from genomic DNA and cDNAs. The PCR mixtures used to clone the entire gene contained: 10–20 ng template, 0.4 µM each primer, 1X PCR buffer, 2 mM $MgSO_4$, 0.2 mM dNTP and 1 unit high fidelity platinum *Taq* (Invitrogen, Burlington, ON, Canada). The reactions were performed under the following conditions: initial denaturation at 94°C for 3 min, 35 cycles with denaturation at 94°C for 30 s, annealing at 55–65°C for 45 s, extension at 68°C for 2–3 min when cDNA as template and for 3–6 min when genomic DNA as template, and final hold at 4°C. PCR products were purified, cloned and sequenced as described above.

Sequence similarity searches were performed using the basic local alignment search tool (BLAST) with default settings (http://www.ncbi.nlm.nih.gov/BLAST). Sequence alignments and phylogenetic analyses were performed by using Clustal W (Thompson et al. 1994) for nucleotide and Clustal X (Thompson et al. 1997) for amino acid with default settings at the web site of the European Bioinformatics Institute (http://www.ebi.ac.uk/clustalw). BOXSHADE (http://www.ch.embnet.org) was used to draw the alignments.

RFLP analysis

Genomic DNA samples (20 µg) from lines of the segregating population were digested with restriction enzymes (30 units of *Eco*RI or *Eco*RV), and fractionated by electrophoresis on 0.8% agarose gels. The gels were stained with ethidium bromide, visualized under UV light and the DNA was transferred onto nylon membranes (Hybond-N^+, Amersham, Oakville, ON, Canada) using protocols recommended by the manufacturer (Boehringer Mannheim, Mannheim, Germany). The forward primer (RFLP-F 5′-GTTGTACATGTCCCTCCATGTA-3′) of the RFLP probe was designed to include the repeated sequence in the 3′-UTR region of the *Zmgc1* gene of the parental line CG62. The forward primer and the reverse primer (RFLP-R 5′-TGGCAGAAGCGACCTTGAATG-3′) amplified a 463 bp genotype-specific fragment from the CG62 that was used as a RFLP probe for the hybridization.

The RFLP probe was labeled with Digoxigenin-11-dUTP using a PCR DIG labeling kit according to the manufacturer's recommendation (Roche Diagnostics GmbH, Mannheim, Germany). The membranes were pre-hybridized overnight at 37–42°C in DIG Easy Hyb solution and hybridized in DIG Easy Hyb solution containing the genotype-specific probe for at least 24 h at 37–42°C according to the instructions of manufacturer (Boehringer Mannheim, Mannheim, Germany). After several washings with 2X SSC at room temperature and 0.5X SSC at 56°C, the hybridization pattern was visualized by chemiluminescence (Roche Diagnostics, Laval, PQ, Canada) and recorded on X-ray film (Kodak Inc, Rochester, NY, USA).

Evaluation of the mapping population and statistical analyses

The parental lines (CG62 and CO387) and 144 lines of the RI population derived from them were previously evaluated for silk and kernel resistance to Gibberella ear rot disease in field trials (Ali et al. 2005). Inbred parental lines were also tested separately for silk and kernel resistance as described by Reid et al. (1996). The experiment was conducted using a randomized complete block design with two replications.

Each block contained all inbred lines, and each line was planted in two rows of 15 plants. All the plants in each paired row were inoculated with a suspension of *F. graminearum* macroconidia. The population mean was compared with the midparental value for both silk and kernel resistance scores (Table 1). Inoculation and scoring of disease severity for field grown plants were performed as described by Ali et al. (2005). The field tests were performed at Ottawa (F4, F6 and F7) in 1999, 2000 and 2001, respectively, and at Tavistock, Ontario (F7) in 2001.

The genetic linkage map was previously constructed using scores for polymorphic RAPD, RFLP, simple sequence repeat (SSR) and sequence-characterized amplified region (SCAR) markers for the individuals from the CG62 × CO387 RI population using MAPMAKER/EXP version 3.0b (Lander et al. 1987) with the Kosambi mapping function (Kosambi 1944). Linkage groups were identified using the "Group" command with a LOD score of 4.0–6.0 and a recombination fraction of 0.4 (Ali et al. 2005). The new guanylyl cyclase derived RFLP markers were added to existing linkage groups with the "Try" command. The guanylyl cyclase RFLP markers were evaluated individually by χ^2 analyses for goodness of fit against a 1:1 segregation ratio at a 0.01 probability level. To determine the locations of the QTL on the map and estimate their phenotypic effects, composite interval mapping (CIM) was performed using QTL Cartographer V2.5 (Wang et al. 2006). Single marker by trait data associations were carried out using PROC GLM (V8.2, SAS Institute, Cary, NC, USA).

Table 1 Mean values of disease severity scores[a] for CO387 (resistant), CG62 (susceptible) and 144 RI lines derived from the CG62 × CO387 cross and parents for following inoculation through silk channels and kernel wounds tested in four environments

Environment	Line	Inoculation method	
		Silk	Kernel
Ottawa 1999	RI	2.9 ± 0.9	3.7 ± 0.9
	CG62 (P1)	5.6	5.3
	CO387 (P2)	2.8	2.1
Ottawa 2000	RI	3.2 ± 1.0	4.1 ± 1.0
	CG62 (P1)	3.7	5.8
	CO387 (P2)	2.8	2.3
Ottawa 2001	RI	3.2 ± 0.9	4.3 ± 1.2
	CG62 (P1)	3.9	6.2
	CO387 (P2)	1.9	2.6
Tavistock 2001	RI	3.4 ± 1.4	4.2 ± 1.2
	CG62 (P1)	4.5	5.5
	CO387 (P2)	1.7	2.8

[a] Visual evaluations of disease severity were made using a rating scale from 1 to 7, where 1 = no visual signs of infection, 2 = 1–3%, 3 = 4–10%, 4 = 11–25%, 5 = 26–50%, 6 = 51–75% and 7 = 76–100% of the ear infected (Reid et al. 1996)

Real time PCR quantification

To study *Zmgc1* gene expression, quantitative real-time PCR was performed using cDNA synthesized from RNA samples from silk tissues of CG62 and CO387 infected with *F. graminearum*. A Ribogreen RNA quantitation kit (Molecular Probes, Eugene, OR, USA) and a Wallace Victor microplate reader (Perkin-Elmer Life Sciences, St Laurent, PQ, Canada) with the lamp filter F485 and the emission filter F530 were used to quantify the RNA. Reverse transcription was carried out with 1 µg of total RNA with the Retroscript kit at 50°C for one hour and 92°C for 5 min, following manufacturer's instruction (Ambion, Austin, TX, USA). The analysis was performed with an iCycler (Bio-Rad Laboratories, Mississauga, ON, Canada) equipped with a Real-time Optical Module and a SYBR Green Supermix kit (Bio-Rad, Hercules, CA, USA). Real-time PCR primers (Realtime-F 5′-ACAACAGCAC AACGATGAGCCTGACTAC-3′ and Realtime-R 5′-ATT-TGCGGGCCTCGTCCAAGCTCTTCATTG-3′) were based on exon 6 and exon 8 sequences, respectively, of the *Zmgc1* gene. The realtime PCR product, approximately 150 bp in length, was cloned using a TOPO TA cloning kit (Invitrogen, Burlington, ON, Canada) and introduced into *E. coli* One-Shot competent cells according to the manufacturer's instructions (Invitrogen, Burlington, ON, Canada). After overnight incubation, plasmid DNA was isolated with a Qiagen Miniprep Kit (Qiagen, Mississauga, ON, Canada) and was linearized by digestion with *Hin*dIII (New England Biolabs, Beverly, MA, USA). The linearized plasmid DNA standards and Low DNA Mass Ladder (Invitrogen, Burlington, ON, Canada) were run in a 0.8% agarose gel stained with ethidium bromide. Densitometry was performed using FluorChem™ (Alpha Innotech Corporation, San Leandro, CA, USA) to quantify the linear plasmid standard and it was used to prepare a dilution series (2.5×10^7—2.5 copies) for generating a standard curve by real time PCR. The final 20 µl real time PCR reaction mixture contained 2 µl of plasmid or cDNA sample, 4 nm primers and 10 µl 2X SYBR Green Supermix (Bio-Rad, Hercules, CA, USA). Real-time PCR was performed using a program consisting of: 1 cycle of 95°C for 3 min, followed by 40–50 cycles of 95°C for 15 s, 65°C for 15 s and 72°C for 30 s. Gene copy number was calculated using a standard curve method with regression equations generated by iCyclerIQ™ the on the iCycler. The internal standard used to normalize the results was a fragment amplified with primers derived from the maize 18S rRNA (F: 5′-TAGTT AGCAGGCTGAGGTCTCG;-3′; R: 5′-CTTACCAGGTC CAGACATAGC-3′). To distinguish non-specific amplification from target amplicons, melting curve analyses were performed in which the samples were heated from 50 to 95°C at a heating rate of 0.5°C/s. All three biological

samples for each time interval per genotype were run in triplicate, including samples for the standard curve and no template controls. Results were analyzed using the PROC GLM procedure of SAS after log transformation of the values. The model was a 2-way factorial with treatment and time as the main factors.

Results

Genomic structure of *Zmgc1* gene

Using the RAPD primer BC324, a 1,200 bp fragment (BC324-1400) was amplified from genomic DNA of the susceptible cultivar CG62. This band did not amplify from genomic DNA of the resistant cultivar CO387 (data not shown). BC324-1400 segregated in a 1:1 ratio in the RI population derived from these parental lines ($\chi^2 = 0.704$). The fragment was cloned and sequenced to a develop SCAR marker which, in turn, revealed a 463 bp long sequence with homology to a guanylyl cyclase (EC 4.6.1.2) gene from *Arabidopsis* (data not shown). To characterize more of the DNA around this putative open reading frame (ORF), 6 kb of genomic DNA was cloned downstream and upstream of the RAPD fragment in several steps of genome walking with genomic DNA from CO387 (Fig. 1a).

The ORF of the *Zmgc1* gene (GenBank accession number: DQ372067) was determined by piecing together DNA sequences for the RACE products, the genome walking fragments, and EST fragments (AY110155 and CO531826) (Fig. 1b) using CAP3 (Huang and Madan 1999) and ORF Finder programs (http://www.ncbi.nlm.nih.gov/gorf). The complete and expressed *Zmgc1* gene sequences (including 3′- and 5′-UTR regions) were obtained by amplifying cDNA and genomic DNA, respectively, from CO387 and CG62 (Fig. 1a, b). The genomic DNA clones are approximately 3.3 kb in size. The cDNA clones are 1.3 kb and contain an ORF for a predicted protein of 267 amino acids (Fig. 2). The region upstream of the gene coding sequence is GC-rich and appears to be a TATA-less promoter (Smale 1997).

The *Zmgc1* ORF in the genomic clones consists of nine exons interrupted by eight introns that are evenly distributed throughout the gene. Exon sizes range from 60 to 131 bp while the intron sizes range from 78 to 504 bp (Fig. 1c). The gene sequences at the exon/intron junctions share consensus splice signals such that all the introns begin with a 5′-GT sequence and end with a 3′-AG sequence (Blumenthal and Stewart 1997). Several sequence differences were observed in the UTRs and introns between the CG62 and CO387. In particular, the CG62 allele has a 57-bp sequence in the C-terminal part of the ORF that is repeated in the 3′-UTR (Fig. 3a). The *Zmgc1* ORFs in the cDNAs from the two cultivars are identical except for three conservative base changes: C (CG62) to T (CO387) in exon 3, A (CG62) to C (CO387) in exon 8, and G (CG62) to A (CO387) in exon 9 (Fig. 2). By using a PCR primer that spans the junction between the repeated regions in the 3′-UTR of the CG62-*Zmgc1* gene it was possible to amplify the gene specifically from this parental genotype and from RI lines that contained the repeat (Fig. 3b). However, the segregation ratio for this SCAR (GC324, Fig. 3) in the RI population was skewed toward the CG62 allele (approximately 3:1 ratio).

Comparison with other GCs

The intron/exon organization of *Zmgc1*-CG62 and *Zmgc1*-CO387 is very similar to the *Arabidopsis Atgc1*. Exons 3, 4, 5, 7, and 8 are identical in size in these two species (Fig. 1c), suggesting a high level of conservation in the coding region for this gene across plant families.

The putative ZmGC1 protein is 53% identical and 65% similar to the *Arabidopsis* AtGC1 (GenBank accession number AAM51559). The putative ZmGC1 protein contains a glycine-rich domain in the N-terminal end of the catalytic center (Fig. 4). The glycine-rich domain can be described as G-X(2,3)-G-X(2,3)-G. ZmGC1 also possesses the conserved arginine that is thought to be involved in hydrogen bonding with guanine and a putative PPi-binding arginine in its N-terminal end (Ludidi and Gehring 2003). However, the catalytic center of the putative ZmGC1 protein has nine fewer amino acids compared to the *Arabidopsis* protein (Fig. 4). Similar to AtGC1, the putative ZmGC1 protein does not have any other typical domains of animal GCs, such as the dimerization domain, kinase-homology domain, transmembrane domain, ligand-binding domain and the heme-binding domain that interacts with NO molecules (Lucas et al. 2000).

Clustal analysis of the deduced ZmGC1 amino acid sequence with the GC sequences that were used by Ludidi and Gehring (2003) to identify the *Arabidopsis* GC showed that the two plant sequences are distinct from the rest of the GCs (Fig. 5). The GC from the cyanobacterium *Synechocystis* sp., a photoautotrophic, gram-negative, photosynthetic eubacterium (Williams 1988) was the closest to the plant GCs. Human (*Homo sapiens*) and frog (*Xenopus laevis*) GCs were the least similar to ZmGC1 (Fig. 5).

Genetic mapping and association of *Zmgc1* with Gibberella ear rot resistance

Southern blots of genomic DNA probed with a portion of the *Zmgc1* gene that corresponds to most of the original BC324-1400 RAPD fragment revealed multiple bands

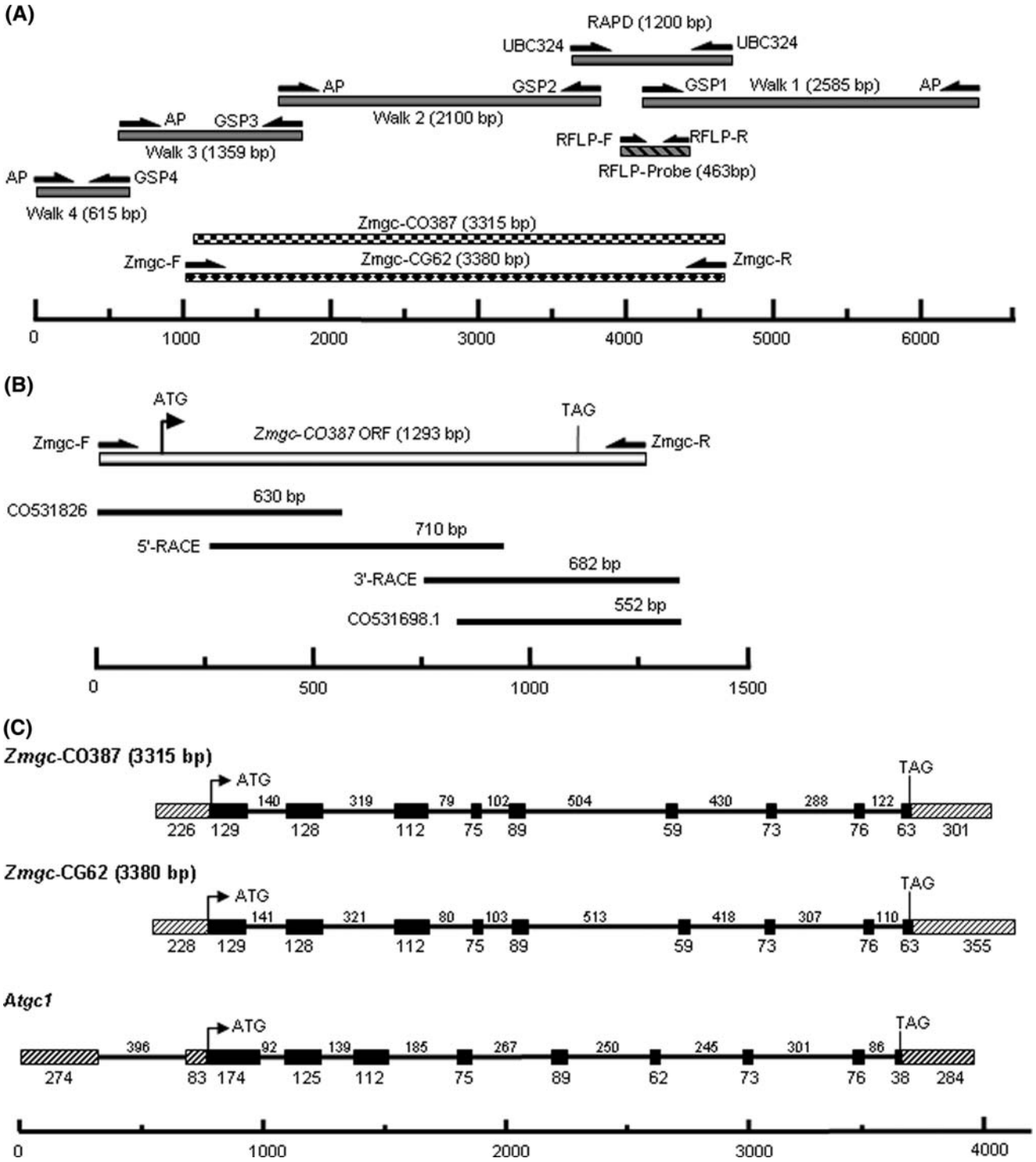

Fig. 1 Cloning of the maize guanylyl cyclase (*Zmgc1*) and comparison of *Zmgc1* alleles to *Arabidopsis Atgc1*. **a** Genome walking steps used to clone the full length *Zmgc1* gene. The primers GSP1 and GSP2 were designed on the basis of the BC324-1400 sequence. After four walking steps using adaptor primer (AP) and gene specific primers (GSP1 GSP2, GSP3 and GSP4) a total of 6.2 kb of genomic sequence was obtained from genotype CO387. ORF fragments were amplified from CG62 (3380 bp) and CO387 (3315 bp) based on primers ZMGC1-F 5′-GTGTCCACCGCGCTCGCCCCCTGCT-3, and *Zmgc1*-R 5′-AGAGGAGCATGATTTTAATTTTA-3′. The RFLP probe was amplified using primers RFLP-F and RFLP-R. **b** RACE and EST (CO531826 and CO531698) fragments used to assemble a full length *Zmgc1* ORF. **c** Comparison of genomic structure of *Zmgc1*-CO387 and *Zmgc1*-CG62 with *Atgc1*. The mRNA sequence (NM_120675) that was identical to *Atgc1* cDNA and At5g05930 was used to construct the genomic structure of *Atgc1*. *Horizontal lines with numbers* indicate introns while *black boxes with numbers* denote exons. Sequences upstream and downstream of the genes are shown with *hatched boxes*

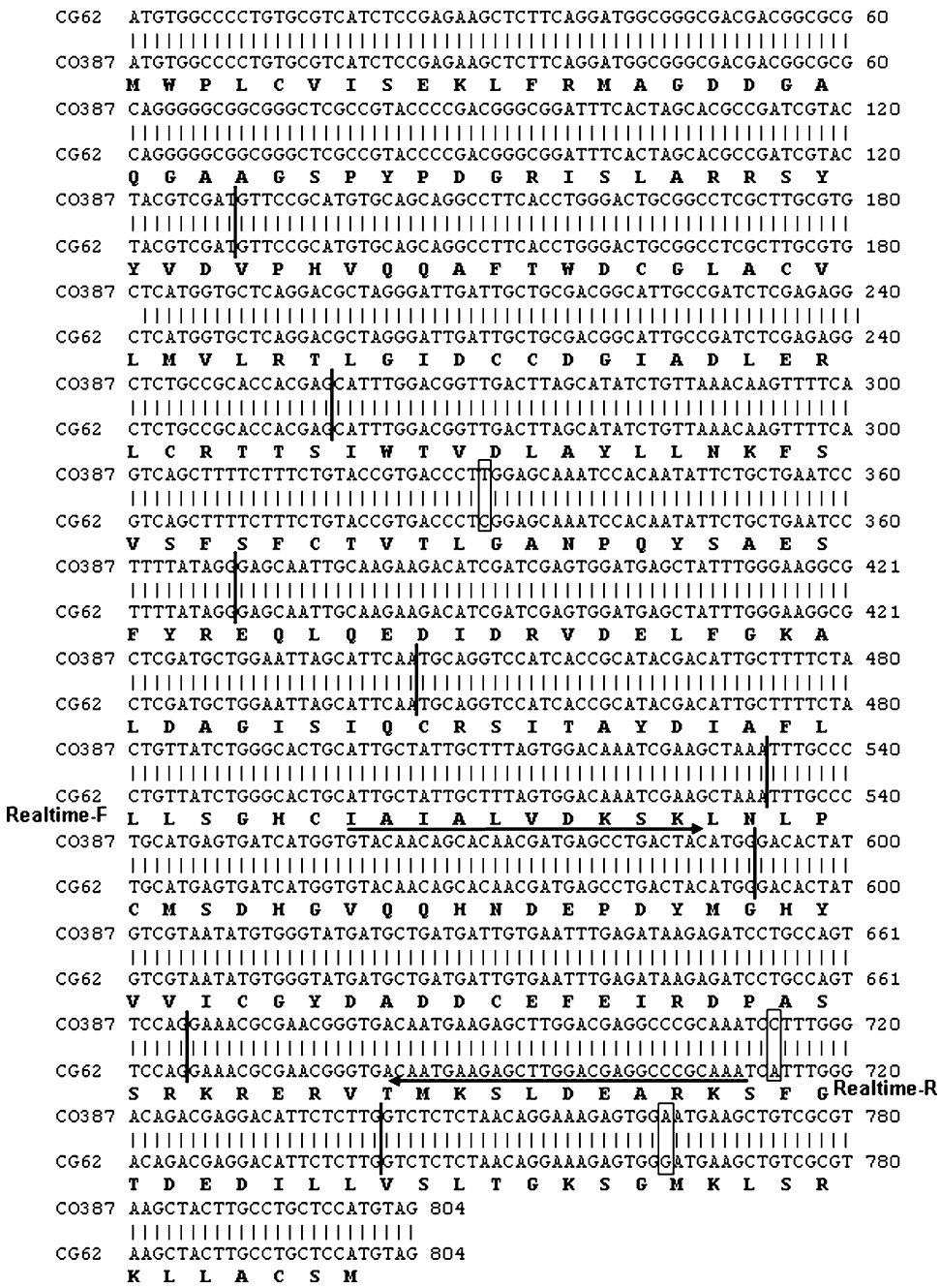

Fig. 2 Comparison of the ORFs of *Zmgc1* CG62 and CO387. The amino acid coding sequence is shown by the one-letter code. The nucleotide differences in exons 3, 8, and 9 are *boxed*. The positions of the primers (Realtime-F and Realtime-R) for real-time PCR are marked by *black arrows*. The intro-exon boundaries are indicated by *black bars*

(Fig. 6a, b), suggesting that GCs exist as a multigene family in maize. The RAPD marker was previously mapped to linkage group 7 using the population of 144 RI lines derived from CG62 and CO387 (Ali et al. 2005). Six polymorphic *Zmgc1* markers were identified following digestion of the same RI population with *Eco*RI (ER1_1 to ER1_5) and *Eco*RV (ER5_1) (Fig. 6a, b). ER1_1 was mapped to the same position as the BC324-1400 marker, which was originally associated with resistance, on linkage group 7 (Ali et al. 2005). This marker (ER1_1) is located between BC324_1400 and umc2332 at a distance of 6 cm from BC324_1400 and 14 cm from umc2332 (Fig. 7). ER1_2 and ER1_4 mapped to chromosome 3 and flanked a QTL for kernel resistance. ER5_1 mapped to linkage group 8 which did not contain resistance QTL in the previous study (Ali et al. 2005).

The mean disease severity scores for CO387 were 2.3 and 2.4 following silk or kernel inoculation, respectively, while CG62 had silk and kernel scores of 4.4 and 5.7, respectively (Table 1; Ali et al. 2005). *Zmgc1* markers, ER1_1 and ER5_1 were significantly associated with the *F. graminearum* resistance (Table 2; Fig. 7) by single marker analysis with the PROC GLM analysis of SAS. ER1_1 was significantly ($P < 0.05$) associated with the resistance in

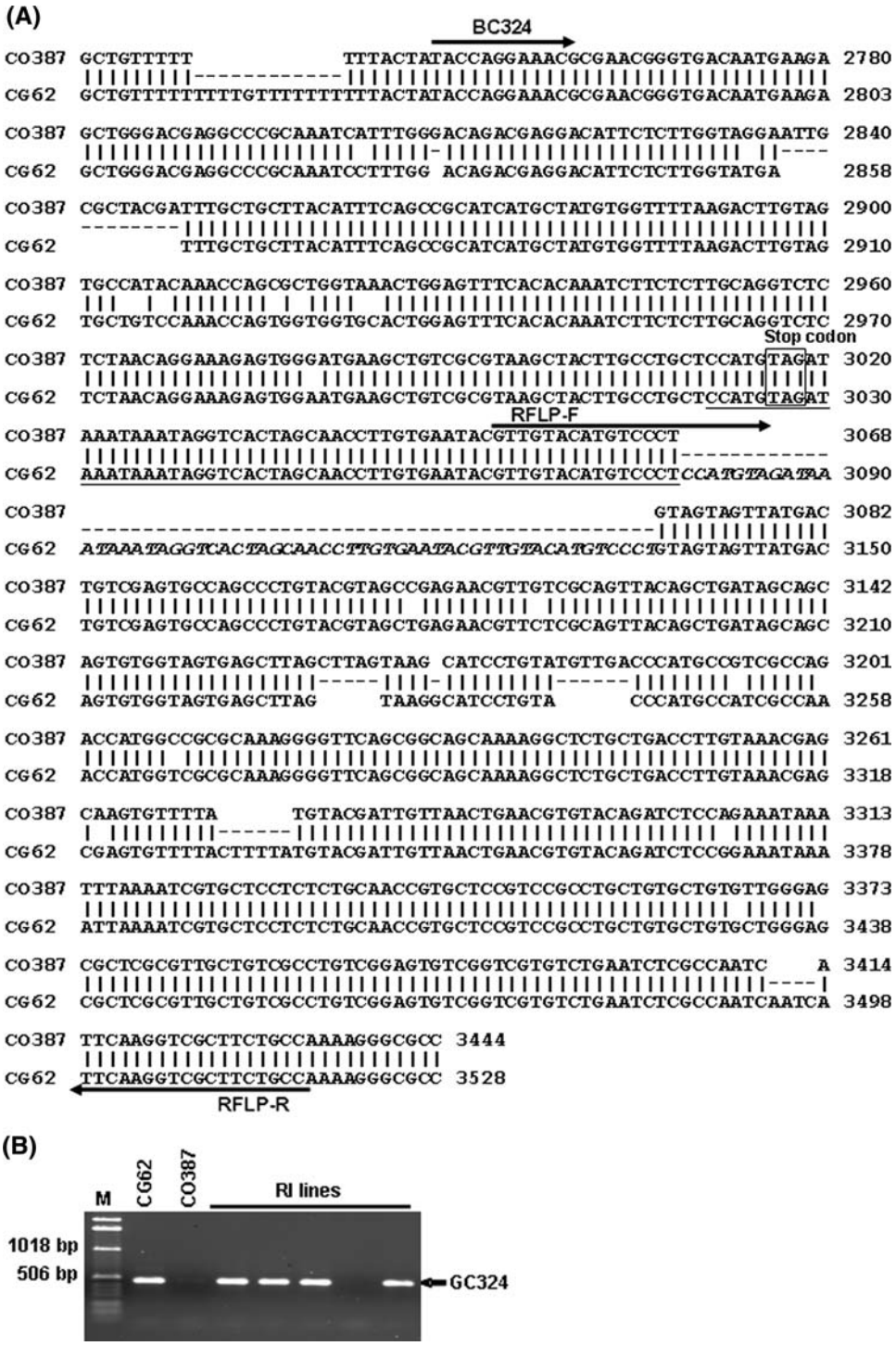

Fig. 3 The 3′-nucleotide sequence alignment of the maize *Zmgc1* gene from CG62 and CO387. **a** RAPD primer BC324 (5′-ACAGGGAACG-3′) and RFLP (RFLP-F 5′-GTTGTACATGTCCCTCCATGTA-3′; RFLP-R 5′-TGGCAGAAGCGACCTTGAATG-3′) are indicated by the *black arrows*. The first copy of the 57 bp repeated sequence in CG62 is *underlined*. The second copy is *italicized*. **b** SCAR marker GC324 This marker amplified only from the CG62 parent and RI lines containing the 57 bp repeat sequence using primers SCAR-F (5′-GTTGTACATGTCCCTCCATGTA-3′) and SCAR-R (5′-TGGCAGAAGCGACCTTGAATG-3′)

more than one environment (Ottawa 1999, Ottawa 2000, Tavistock 2001). Resistance was associated with the allele from CO387 in all cases. A QTL that mapped to the interval ER1_1-umc1407 was detected by composite interval mapping (QTL Cartographer) in two environments and contributed to silk resistance (Ottawa 1999 silk, Tavistock 2001 silk). It accounted for 15.5% of the Tavistock 2001 test variation (silk resistance) with a LOD score of 4.02 and 10.3% of the Ottawa 1999 test variation (silk resistance) with a LOD score 3.03 (Table 2).

ER5_1 was positioned on linkage group 8, 21 cm from molecular marker umc1032 (Fig. 7). Single marker analysis, showed that ER5_1 was significantly ($P < 0.05$) associated with kernel resistance in more than one environment (Ottawa 1999, Ottawa 2000, Tavistock 2001), that the resistant allele was derived from CO387 and it explained

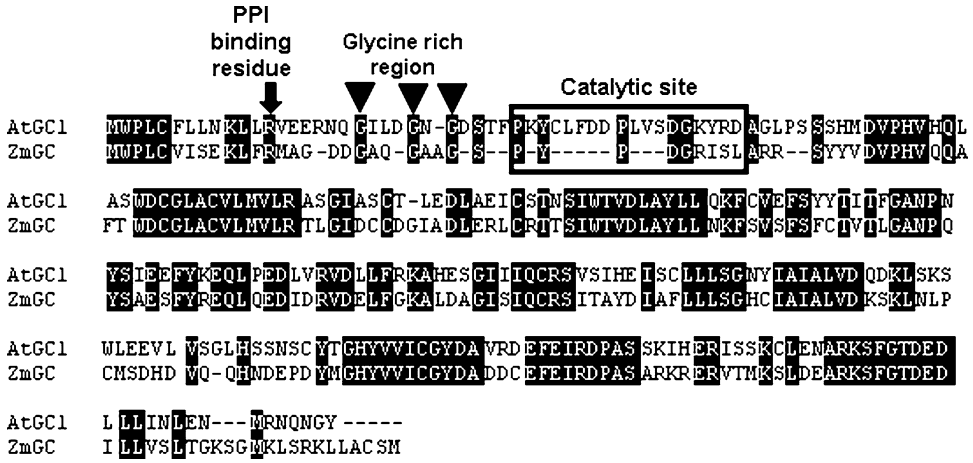

Fig. 4 Alignment of the deduced amino acid of *Zmgc1* with AtGC1 (*A. thaliana*, AAM51559). The postulated catalytic domains of the guanylyl cyclases are *boxed*. The postulated PPi-binding arginine (R) residues and conserved glycines (G) are marked with *black arrows*

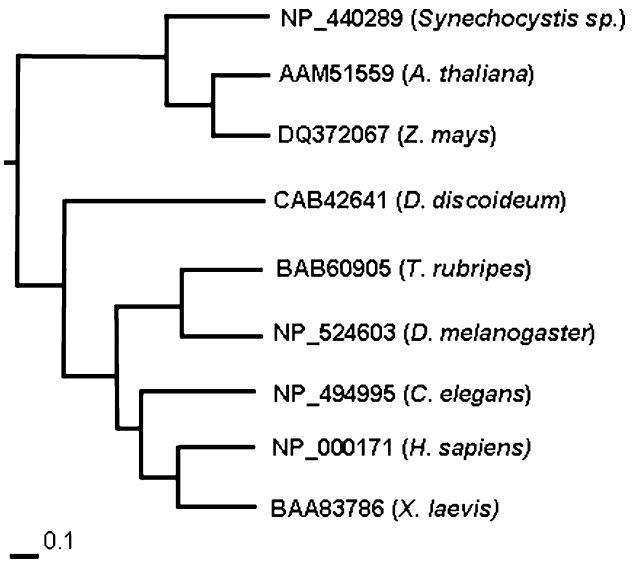

Fig. 5 Clustering analysis of guanylyl cyclases. Amino acid sequences of GCs and putative amino acid sequence of ZmGC1 were aligned with the Clustal W program. The selection of these guanylyl cyclase sequences was based on the catalytic domain searching described by Ludidi and Gehring (2003). GenBank accession numbers for the sequences are *H. sapiens*, NP_000171; *D. melanogaster*, NP_524603; *C. elegans*, NP_494995; *A. thaliana*, AAM51559; *Synechocystis sp*, NP_440289; *T. rubripes*, BAB60905; *X. laevis*, BAA83786; *D. discoideum*, CAB42641; *Z. mays*, DQ372067. The *scale bar* represents an evolutionary distance of 0.1 amino acid substitution per residue

between 7.3 and 12.2% of the phenotypic variation. However, composite interval mapping did not detect any resistance QTL in this region.

Single marker analyses with RFLP markers ER1_2 and ER1_4 showed that they were not significantly associated with the resistance. However, the molecular marker phi37411 that is located between ER1_2 and ER1_4 was significantly associated with disease resistance ($P = 0.04$, $R^2 = 4.4$). The QTL in the interval ER1_2-phi374118 had a peak LOD score of 2.2 and accounted for 13% of the kernel resistance variation in the Ottawa 2001 test (Fig. 7, Ali et al. 2005).

With marginal linkage, RFLP markers ER1_3 and ER1_5 were mapped to linkage group 8 and linkage group 2, respectively. However, more markers are needed to saturate the neighboring regions. Neither was associated with resistance to *F. graminearum* infection (data not shown).

Zmgc1 gene expression

Zmgc1 transcripts were detected by RT-PCR in the several tissues including leaf, silk, and root (data not shown) suggesting that the gene was constitutively expressed in maize. Quantitative real-time PCR was employed to evaluate *Zmgc1* transcript levels in ear tissue samples harvested at different times (0–240 h after *F. graminearum* inoculation. The normalized *Zmgc1* to 18S rRNA transcript ratio was higher in the resistant (CO387) tissue than in the tissue of the susceptible genotype (CG62) both before and after the pathogen inoculation. (Fig. 8). The SAS GLM analysis indicated that the overall differences between genotypes were significant ($P = 0.005$) and the changes over time were also statistically significant ($P = 0.0001$; genotype × time interactions were not statistically significant). The *Zmgc1* relative transcript abundance in CO387 increased almost sevenfold at 24 h after inoculation compared to its 1 h level and then gradually declined. The transcript level in CG62 reached its peak 48 h after inoculation. Ten days after inoculating with the pathogen, *Zmgc1* transcripts levels were significantly lower in both genotypes. In particular, very few transcript copies were detected in the susceptible genotype (CG62) compared to the resistant genotype (CO387) because of the extensive necrosis in the silk tissue of the former.

Discussion

To the best of our knowledge, this is the first report of a guanylyl cyclase-like gene in *Z. mays*. The similarity of the

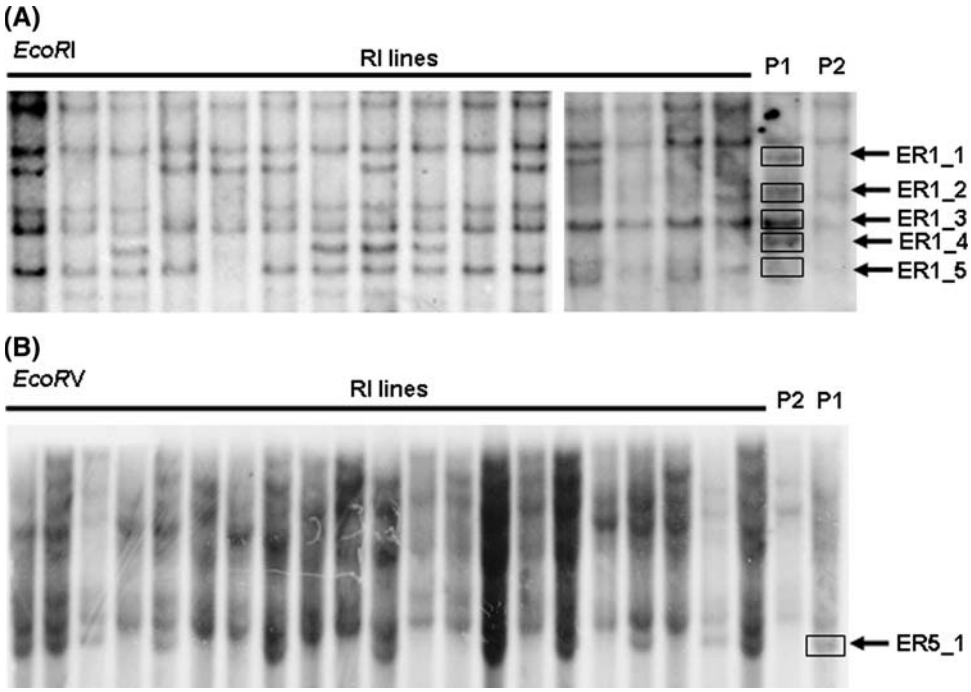

Fig. 6 Restriction fragment patterns of selected RI lines hybridized with the 3′-UTR region of *Zmgc1*-CG62. The probe was amplified using primers RFLP-F 5′-GTTGTACATGTCCCTC-CATGTA-3′ and RFLP-R 5′-TGGCAGAAGCGACCT-TGAATG-3′labeled with DIG. (**a**). The lines were digested with *Eco*R-I and five bands were scored as separate markers (*Eco*R1_1, *Eco*R1_2, *Eco*R1_3, *Eco*R1_4, and *Eco*R_5). The polymorphic bands are indicated by *arrows* on the *right*. Portions of two membranes are shown (**b**). The RI population was digested with *Eco*RV and one band was scored (*Eco*R5_1, indicated by *arrow*); *RI* recombinant inbred lines, *P1* CO387 parent; *P2* CG62 parent

overall gene structure and putative amino acid sequence to the previously characterized GC from *Arabidopsis* (*Atgc1*) is striking. Both genes have the same number of introns and five of the nine exons are the same size. The greatest similarities between AtGC1 and ZmGC1 are in their catalytic and kinase-like domains. Unlike animal GCs, the catalytic domains in the maize and *Arabidopsis* genes are located in their N-termini. Both *Arabidopsis* AtGC1 and maize ZmGC1 have a glycine-rich motif. In animal GCs, the glycine-rich motif may function like the P-loop of GTP-binding proteins by providing flexibility to the part of protein that interacts with the phosphate group in GTP (Saraste et al. 1990). Both GCs lack extracellular domains. Also, the upstream regions of the *Zmgc1* and *Atgc1* lack TATA box sequences (Ludidi and Gehring 2003). A difference between ZmGC1 and AtGC1 is the putative catalytic center of the maize protein has nine fewer amino acids. It is not clear whether this would alter enzyme activity or substrate dependence.

Overall the strong similarities between the maize and *Arabidopsis* genes with regard to their sequence and structure suggest that they might belong to a conserved gene family across plant species. In the GC superfamily, ZmGC1, AtGC1, and *Synechocystis* GC are most closely related. The close relationship between the two plant GCs and their association with the GC from the cyanobacterium *Synechocystis* suggests that all three sequences have a common ancestor and that perhaps the plant genes may be derived from an endosymbiont ancestor of the chloroplast.

We identified six GC RFLP markers that mapped to four linkage groups of maize and showed that GC markers on linkage group 7 and 8 were significantly associated with resistance to *F. graminearum*, but jointly explained less than 20% of the variation in disease resistance. This dispersed model of resistance is in accordance with earlier findings, including our own QTL analyses (Ali et al. 2005), that *F. graminearum* resistance is a quantitative, multigenic trait in maize. Hart et al. (1984) suggested that additive gene effects condition resistance. Reid et al. (1992, 1994) found the resistance following silk inoculation to be largely influenced by a single major gene whose expression was sensitive to environmental conditions. Chungu et al. (1996) estimated that 5 to 14 genes with largely additive effects controlled kernel resistance to ear rot in maize.

Gene duplication, deletion, and conversion are thought to happen very often at disease resistance loci (Schnable et al. 1998). However, in the present study, in spite of the three SNPs that were detected in the exons of the genes, the predicted proteins from the two cultivars are identical. These results suggest that the evolution of the GC gene has been under tight regulation. The largest difference that was observed was the 57 bp sequence that was repeated in the 3′-UTR of the gene from the susceptible parent GC62. UTRs are thought to play crucial roles in post-transcriptional regulation of gene expression, such as, modulation of the transport of mRNA out of the nucleus, subcellular localization and stability (van der Velden and Thomas 1999; Jansen 2001; Bashirullah et al. 2001). Modifications in 3′ UTR-mediated functions may change the expression of genes and can lead to abnormal gene function (Conne et al. 2000). Only two alleles of the GC gene and mRNA were identified and only one allotype of the

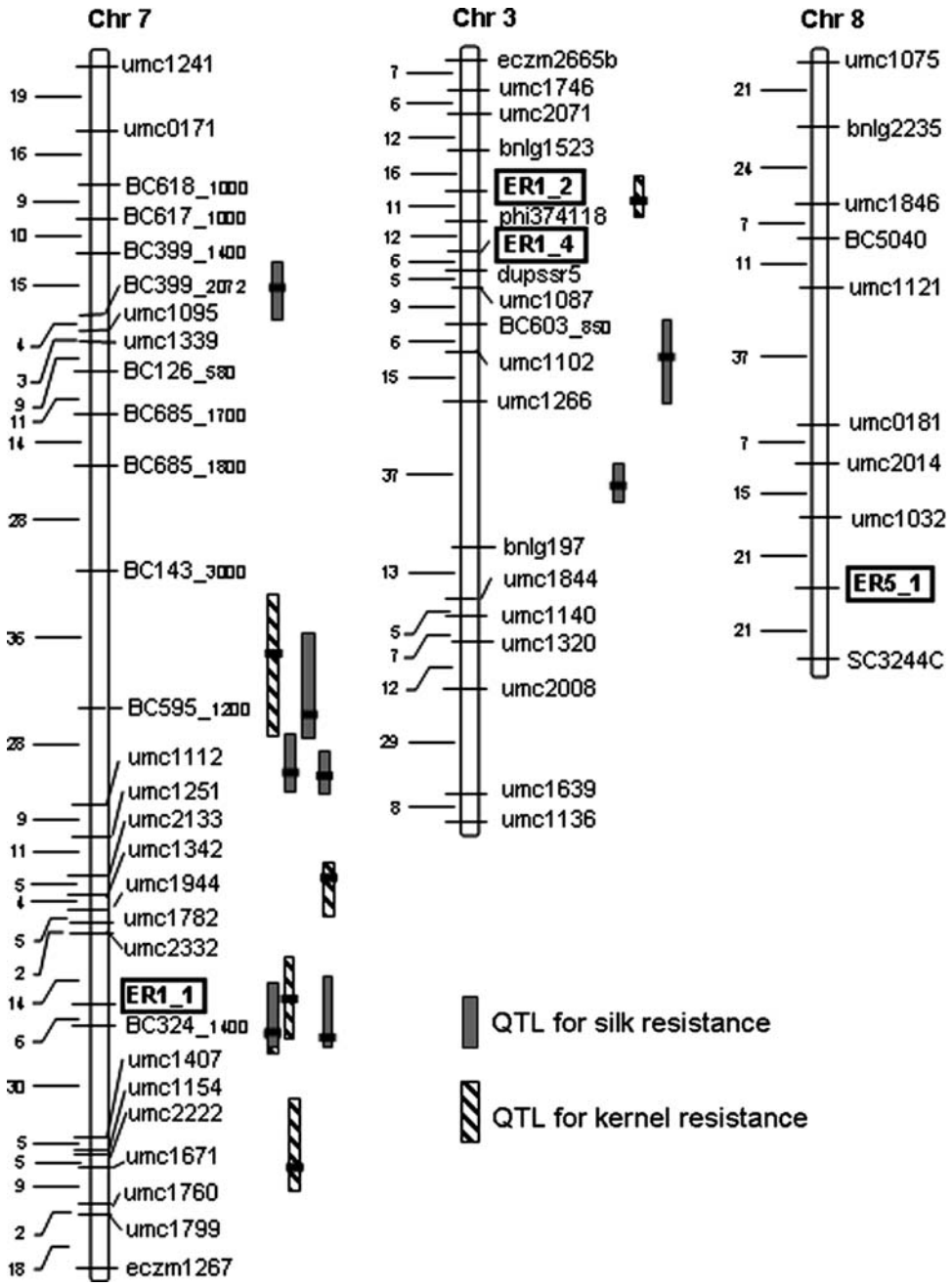

Fig. 7 Map positions of the guanylyl cyclase markers on maize chromosomes. The genetic map was generated from segregation data of molecular markers in the CG62 × CO387 RI population (Ali et al. 2005) combined with the GC RFLP segregation data generated in this study. Recombination distances between the markers are indicated in cM on the *left side* of the chromosome and the marker names are on the *right* side of the chromosome. The GC RFLP markers are *boxed*. *Vertical bars* indicate QTL regions with a LOD > 2.0. *Horizontal lines* on the bars indicate the positions of the QTL peaks. QTL for silk resistance are marked by *solid bars* while QTL for kernel resistance are marked by *hatched bars*. QTL detected in more than one environment are indicated by *multiple bars*

putative amino acid sequence was inferred. More homologous sequences may be detected in a wider selection of the *Z. mays* germplasm or by probing under low stringency. The differences between the two alleles may result from either post-transcriptional or translational changes in expression.

Although the original RAPD marker segregated 1:1 in the population and mapped to a single location the SCAR marker that was developed for the GC sequence it contained has a 3:1 (present:absent) distribution. The skewed distribution of the SCAR marker (GC324) in the mapping population was likely the result of priming from multiple copies of the GC gene within the maize genome as demonstrated by the RFLP blots.

In plants, cGMP modulates expression of many defense and stress related pathways gene (Bowler et al. 1994). A few studies have reported an involvement of guanylyl cyclase gene expression with disease resistance (Durner et al. 1998; Klessig et al. 2000). It is not known whether the maize guanylyl cyclase plays direct roles in perception of host stimuli or has roles in signal processing. Gibberella ear rot infections usually occur when the cool weather precedes wet and warm condition during flowering. It would be interesting to determine if the low temperature affects the abundance of

Table 2 QTL effects of guanylyl cyclase-based RFLP markers for resistance to *Fusarium graminearum* infection in maize detected by single marker (SM) analysis and composite interval mapping (CIM) compared with the RAPD marker BC324_1400

Marker[a]	Trait	Environment	SM analysis		CIM analysis		
			Variance (%)[b]	*P* value[c]	Variance (%)[d]	Additive effect[e]	LOD[f]
ER1_1	Silk	Ottawa 1999	9.5	0.0002	10.3	0.28	3.03
BC324_1400	Silk	Ottawa 1999	9.6	0.001	15.9	0.35	3.23
ER1_1	Silk	Ottawa 2000	4.4	0.0131	–	–	–
BC324_1400	Silk	Ottawa 2000	4.4	0.01	–	–	–
ER1_1	Silk	Tavistock 2001	6.5	0.0176	15.5	0.57	4.02
BC324_1400	Silk	Tavistock 2001	7.4	0.01	32.6	0.82	5.0
ER5_1	Kernel	Ottawa 2000	7.4	0.0104	–	–	–
	Kernel	Ottawa 2001	7.3	0.0233	–	–	–
	Kernel	Tavistock 2001	12.2	0.0072	–	–	–

[a] Marker linked to a QTL for a specific trait/location

[b] Variance (R^2) explained by a marker (QTL) estimated by single marker analysis using ANOVA

[c] Probability value for significance

[d] Variance (R^2) explained by a QTL estimated by CIM

[e] Additive genetic effects estimated by CIM (QTL Cartographer 2.5) and the values indicate the amount of disease severity reduced by the CO387 (resistant parent) alleles. The amount of disease severity was determined based on the disease severity scoring scale of 1 to 7

[f] LOD likelihood score for a QTL at the position of the linked specific marker

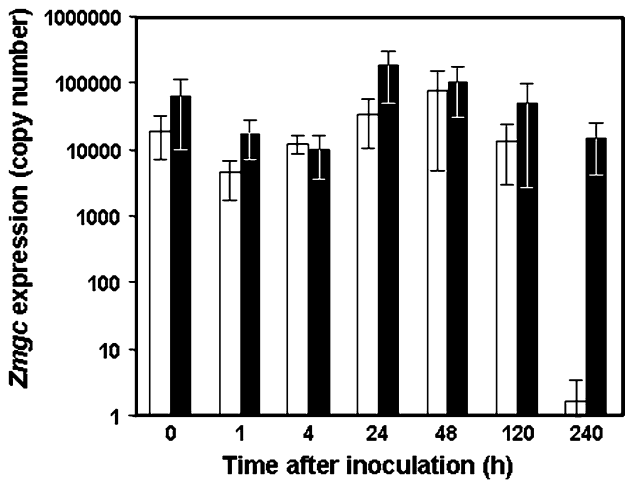

Fig. 8 *Zmgc1* transcript abundance in silk tissue after *F. graminearum* inoculation as determined by real-time PCR. The *Zmgc* copy number values were normalized relative to 18S rRNA. The transcript abundance values for *Zmgc* in CO387 (*filled square*) and CG62 (*open square*) are indicated; $n = 3$, means ± SE are indicated

cGMP transcript in maize and how the *Zmgc1* gene products interact with other host–pathogen interaction gene products.

The results of our gene expression experiment support the hypothesis that GCs are involved in resistance because the overall abundance of the *Zmgc1* gene transcript was higher in the silk tissue of the resistant genotype (CO387) than in the susceptible genotype (CG62) during most stages of infection by *F. graminearum*. In addition, *Zmgc1*-CO387 gene transcript levels at 24 h were seven fold higher than the levels 1 h after the inoculation, suggesting that the pathogen infection can induce GC expression. The large drop in expression in the infected tissue in the susceptible line at 240 h could be attributed to the extensive cell death that occurred in this tissue. Since we used primers that may not distinguish the multiple transcripts that might result from the expression of a multi-gene family, even greater differences might be apparent with gene specific primers.

In conclusion, we have cloned and characterized a guanylyl cyclase-like gene from maize, mapped multiple copies of this gene, described polymorphisms between alleles in resistant and susceptible maize lines and shown that it is significantly associated with *F. graminearum* resistance using QTL analyses and gene expression studies in tissues challenged with the pathogen.

Acknowledgments This work was supported by the Ontario Corn Producers, the Ontario Corn Consortium (including the Ontario Pork Producers, Pioneer Hi-Bred, Syngenta Seeds Canada, Inc), the Ontario Ministry for Food Agriculture and Rural Affairs, The Ontario Research Enhancement Program, Canadapt, the Federation des Producteurs de Cultures Commerciales du Quebec, the Natural Sciences and Engineering Research Council of Canada and Agriculture and Agri-Food Canada. Dr. Rob Gulden and Angela Hill are gratefully acknowledged for their assistance with real time analyses and the preparation of the manuscript, respectively.

References

Ali L, Taylor J, Liu J, Sun G, William M, Kasha K, Reid L, Pauls KP (2005) Molecular mapping of QTLs for resistance to Gibberella ear rot in corn caused by *Fusarium graminearum*. Genome 48:521–533

Bashirullah A, Cooperstock RL, Lipshitz HD (2001) Spatial and temporal control of RNA stability. Proc Natl Acad Sci USA 98:7025–7028

Berridge MJ (1993) Cell signaling. A tale of two messengers. Nature 365:388–389

Bily AC, Reid LM, Taylor JH, Johnston D, Malouin C, Burt AJ, Bakan B, Regnault-Roger C, Pauls KP, Arnason JT, Philogène BJR (2003) Dehydrodimers of ferulic acid in maize grain pericarp and aleurone: resistance factors to *Fusarium graminearum*. Phytopathology 93:712–719

Blumenthal T, Stewart K (1997) RNA processing and gene structure. In: Riddle D, Blumenthal T, Meyer B, Priess J (eds) *C. elegans* II. Cold Spring Harbor Laboratory, Plainview, pp 117–145

Bowler C, Neuhaus G, Yamagata H, Chua NH (1994) Cyclic GMP and calcium mediate phytochrome phototransduction. Cell 77:73–81

Christensen CM, Meronuck RA (1986) Quality maintenance in stored grains and seeds. University of Minnesota, Minneapolis

Chungu C, Mather DE, Reid LM, Hamilton RI (1996) Inheritance of kernel resistance to *Fusarium graminearum* in maize. J Heredity 87:382–385

Conne B, Stutz A, Vassalli JD (2000) The 3′ untranslated region of messenger RNA: a molecular 'hotspot' for pathology? Nat Med 6:637–641

Durner J, Wendehenne D, Klessig DF (1998) Defense gene induction in tobacco by nitric oxide, cyclic GMP and cyclic ADP-ribose. Proc Natl Acad Sci USA 95:10328–10333

Dzeja C, Hagen V, Kaupp UB, Frings S (1999) Ca^{2+} permeation in cyclic nucleotide-gated channels. EMBO J 18:131–144

Garbers DL, Lowe DG (1994) Guanylyl cyclase receptors. J Biol Chem 269:30741–30744

Greenhalgh R, Neish GA, Miller JD (1983) Deoxynivalenol, acetyl deoxynivalenol, and zearalenone formation by Canadian isolate of *Fusarium graminearum* on solid substrates. Appl Environ Microbiol 46:625–629

Hart LP, Gendloff E, Rossman EC (1984) Effect of corn genotypes on ear rot infection by *Gibberella zeae*. Plant Dis 68:296–298

Hoisington DA, Khairallah MM, Gonzales-de-Leon D (1994) Laboratory protocols. CIMMYT Applied Molecular Genetics Laboratory. CIMMYT, Hisfoa

Huang X, Madan A (1999) CAP3: a DNA sequence assembly program. Genome Res 9:868–877

Hurley JH (1998) The adenylyl and guanylyl cyclase superfamily. Curr Opin Struct Biol 8:770–777

Jansen RP (2001) mRNA localization: message on the move. Nat Rev Mol Cell Biol 2:247–256

Klessig DF, Durner J, Noad R, Navarre DA, Wendehenne D, Kumar D, Zhou JM, Shah J, Zhang S, Kachroo P, Trifa Y, Pontier D, Lam E, Silva H (2000) Nitric oxide and salicylic acid signaling in plant defense. Proc Natl Acad Sci USA 97:8849–8855

Kosambi DD (1944) The estimation of map distance from recombination values. Ann Eugen 12:172–175

Lander ES, Green P, Abrahamson J, Barlow A, Daly MJ, Lincoln SE, Newburg L (1987) MAPMAKER: an interactive computer package for constructing primary genetic linkage maps of experimental and natural populations. Genomics 1:174–181

Lee EA, Good B, Chakravarty R, Kannenberg L (2001) Corn inbred lines CG60 and CG62. Can J Plant Sci 81:453–454

Levine A, Pennell RI, Alvarez ME, Palmer R, Lamb C (1996) Calcium-mediated apoptosis in a plant hypersensitive disease resistance response. Curr Biol 6:427–437

Lucas KA, Pitari GM, Kazerounian Ruiz-Stewart IS, Park J, Schulz S, Chepenik KP, Waldman SA (2000) Guanylyl cyclases and signaling by cyclic GMP. Pharmacol Rev 52:375–413

Ludidi N, Gehring C (2003) Identification of a novel protein with guanylyl cyclase activity in *Arabidopsis thaliana*. J Biol Chem 278:6490–6494

McDowell JM, Woffenden BJ (2003) Plant disease resistance genes, recent insights and potential applications. Trends Biotechnol 21:178–183

McMullen M, Jones R, Gallenberg D (1997) Scab of wheat and barley: a re-emerging disease of devastating impact. Plant Dis 81:1340–1348

Mirocha CJ, Pathre SV, Schauerhamer B, Christensen CM (1976) Natural occurrence of *Fusarium* toxins in feedstuff. Appl Environ Microbiol 32:553–556

Molto GA, Gonzalez HHL, Resnik SL, Gonzalez AP (1997) Production of trichothecenes and zearalenone by isolates of *Fusarium* ssp. from Argentinean maize. Food Addit Contam 14:263–268

Pe ME, Gianfranceschi L, Taramino G, Tarchini R, Angelini P, Dani M, Binelli G (1993) Mapping quantitative trait loci (QTLs) for resistance to *Gibberella zeae* infection in maize. Mol Gen Genet 241:11–16

Reid LM, Hamilton RI (1996) Effect of inoculation position, timing, macroconidial concentration, and irrigation of resistance of corn to *Fusarium graminaerum* infection through kernels. Can J Plant Pathol 18:279–285

Reid LM, Mather DE, Hamilton RI, Bolton AT (1992) Genotypic differences in the resistance of cornsilk to *Fusarium graminearum*. Can J Plant Pathol 14:211–214

Reid LM, Mather DE, Bolton AT, Hamilton RI (1994) Evidence for a gene for silk resistance to *Fusarium graminearum* Schw. ear rot of maize. J Hered 85:118–121

Reid LM, Hamilton RI, Mather DE (1996) Screening maize for resistance to Gibberella ear rot. Agriculture and Agri-food Canada Technical Bulletin. 1996–5E, 40pp

Ryals JA, Neuenschwander UH, Willits MG, Molina A, Steiner HY, Hunt MD (1996) Systemic acquired resistance. Plant Cell 8:1809–1819

Saraste M, Sibbald PR, Wittinghofer A (1990) The P-loop—a common motif in ATP- and GTP-binding proteins. Trends Biochem Sci 15:430–434

Schaap P (2005) Guanylyl cyclases across the tree of life. Front Biosci 10:1485–1498

Schnable PS, Hsia AP, Nikolau B (1998) Genetic recombination in plants. Curr Opin Plant Biol 1:123–129

Smale ST (1997) Transcription initiation from TATA-less promoters within eukaryotic protein-coding genes. Biochem Biophys Acta 1351:73–88

Stuber CW, Lincoln SE, Wolff DW, Helentjaris T, Lander ES (1992) Identification of genetic factors contributing to heterosis in a hybrid from two elite corn inbred lines using molecular markers. Genetics 132:823–839

Sutton JC (1982) Epidemiology of wheat head blight and corn ear rot caused by *Fusarium graminearum*. Can J Plant Pathol 4:195–209

Tanksley SD, Nelson JC (1996) Advanced backcross QTL analysis: a method for the simultaneous discovery and transfer of valuable QTLs from unadapted germplasm into elite breeding lines. Theor Appl Genet 92:191–203

Thompson D, Garbers D (1995) Dominant negative mutations of the guanylyl cyclase—a receptor, extracellular domain deletion and catalytic domain point mutations. J Biol Chem 270:425–430

Thompson JD, Higgins DG, Gibson TJ (1994) CLUSTAL W: improving the sensitivity of progressive multiple sequence alignment through sequence weighting, position-specific gap penalties and weight matrix choice. Nucleic Acids Res 22:4673–4680

Thompson JD, Gibson TJ, Plewiak F, Jeanmougin F, Higgins DG (1997) The CLUSTAL_X windows interface: flexible strategies for multiple sequence alignment aided by quality analysis tools. Nucleic Acids Res 24:4876–4882

van der Velden AW, Thomas AA (1999) The role of the 5′ untranslated region of an mRNA in translation regulation during development. Int J Biochem Cell Biol 31:87–106

Wang S, Basten J, Zeng Z-B (2006) Windows QTL Cartographer 2.5. Department of Statistics. Raleigh, NC North Carolina State University http://statgen.ncsu.edu/qtlcart/WQTLCart.htm

Williams JGK (1988) Construction of specific mutations in photosystem II photosynthetic reaction center by genetic engineering methods in *Synechocystis* 6803. Meth Enzymol 167:766–778

Xiao J, Li J, Yuan L, Tanksley SD (1996) Identification of QTLs affecting traits of agronomic importance in recombinant inbred population derived from a subspecific cross. Theor Appl Genet 92:230–244

Young ND (1999) A cautiously optimistic vision for marker-assisted breeding. Mol Breed 6:505–510

Yousef GG, Juvik JA (2001) Comparison of phenotypic and marker-assisted selection for quantitative traits in sweet corn. Crop Sci 41:645–655

Yu S, Avery L, Baude E, Garbers DL (1997) Guanylyl cyclase expression in specific sensory neurons: a new family of chemosensory receptors. Proc Natl Acad Sci USA 94:3384–3387